Hot, metastable hydronium ion in the Galactic center: Formation pumping in X-ray irradiated gas?

Dariusz C. Lis[1,*], Peter Schilke[2], Edwin A. Bergin[3], Martin Emprechtinger[1] and the HEXOS Team[†]

[1] *Cahill Center for Astronomy and Astrophysics 301-17, California Institute of Technology, Pasadena, CA 91125, USA*
[2] *I. Physikalisches Institut, Universität zu Köln, Zülpicher Str. 77, 50937 Köln, Germany*
[3] *Department of Astronomy, University of Michigan, 500 Church Street, Ann Arbor, MI 48109, USA*

With a 3.5-meter diameter telescope passively cooled to ∼80 K and a science payload comprising two direct detection cameras/medium resolution imaging spectrometers, PACS and SPIRE, and a very high spectral resolution heterodyne spectrometer, HIFI, the Herschel Space Observatory is providing extraordinary observational opportunities in the 55–670 μm spectral range. HIFI has opened for the first time to high-resolution spectroscopy the submillimeter band that includes the fundamental rotational transitions of interstellar hydrides, the basic building blocks of astrochemistry. We discuss a recent HIFI discovery of metastable rotational transitions of the hydronium ion (protonated water, H_3O^+), with rotational level energies up to 1200 K above the ground state, in absorption towards Sagittarius B2(N) in the Galactic center. Hydronium is an important molecular ion in the oxygen chemical network. Earlier HIFI observations have indicated a general deficiency of H_3O^+ in the diffuse gas in the Galactic disk. The presence of hot H_3O^+ towards Sagittarius B2(N) thus appears to be related to the unique physical conditions and the widespread presence of abundant H_3^+ in the Central Molecular Zone. The high rotational temperature characterizing the population of the metastable levels may be indicative of H_3O^+ formation pumping in molecular gas irradiated by X-rays emitted by the Galactic center black hole.

Key words: astrochemistry – ISM: abundances – ISM: molecules – molecular processes – submillimetre: ISM.

1. Introduction

The submillimeter band, broadly defined as a decade of wavelengths between 1 mm and 100 μm, gives access to cold, dust enshrouded objects that are often hidden from view at shorter wavelengths. Dust continuum sources with temperatures of order 30 K peak near 100 μm. In colder sources, such as prestellar cores before the onset of star formation, the emission is shifted to

* dcl@caltech.edu
† http://www.hexos.org/team.php

Phil. Trans. R. Soc. A 1–12; doi: 10.1098/rspa.XXXXXXXX
Received 9 February 2012; Accepted

even longer wavelengths. A complex network of chemical reactions takes place in these cold environments, including both gas-phase and grain-surface processes. High-resolution heterodyne techniques provide velocity-resolved ($R \gtrsim 10^6$) spectra of the rotational lines of abundant gas-phase molecules. Such observations give invaluable information about the chemical composition, kinematics (infall, outflow, rotation) and the physical conditions (temperature, density, UV field intensity, ionization fraction) at the onset of star formation. The line forest of heavy organic species that dominates the line spectrum at longer millimeter wavelengths gradually gives way to fundamental rotational transitions of light hydrides and deuterides in the submillimeter. Atomic fine structure lines of abundant elements: C, O, and N, neutral or ionized, are also present and are important coolants of the gas.

The Herschel Space Observatory (Pilbratt et al. 2010) is the fourth ESA cornerstone mission, the first space facility to completely cover the 60–670 μm spectral range. It consists of a 3.5-m diameter telescope, passively cooled to $\sim$80 K, in a Lissajous orbit around the Lagrangian point L2, behind the Moon—a very stable and low-background orbit. The satellite was launched by Ariane 5 on May 14, 2009 from the Centre Spatial Guyanais in Kourou, French Guiana. It carries three cryogenically cooled instruments: two imaging cameras, PACS and SPIRE, both using bolometer detectors, and the heterodyne instrument, HIFI (de Graauw et al. 2010). HIFI covers the wavelength range 625–240 μm using state-of-the art SIS mixers, as well as 212–157 μm using HEB mixers. The instrument has a wide instantaneous IF bandwidth (4 GHz in two polarizations for SIS mixers and 2.4 GHz in two polarizations for HEB mixers), high frequency resolution (1 MHz over the full IF band and up to 140 kHz over a portion of the band), and near-quantum limit sensitivity.

The HIFI science can be broadly described as the "Life Cycle of Gas and Dust". One of the main science themes are unbiased spectral line surveys, which provide a complete census of molecules in star-forming regions. The fundamental rotational transitions of light hydrides and deuterides that dominate the submillimeter spectrum often have very high critical densities and the excited energy levels are difficult to populate by collisions at the typical conditions characteristic of the interstellar medium. However, the dust continuum flux steeply increases at short submillimeter wavelengths (Fig. 1). This offers an opportunity to probe even relatively diffuse regions, characterized by several magnitudes of visual extinction, by means of absorption spectroscopy. Lines of sight towards distant dust continuum sources, such as Sagittarius B2 in the Galactic center, often intersect several Galactic spiral arms, thus allowing detailed investigations of the physics and chemistry of the foreground gas in clouds with a wide range of physical conditions. The Herschel guaranteed time key program HEXOS (*Herschel/HIFI observations of EXtra-Ordinary Sources: The Orion and Sagittarius B2 starforming regions*; Bergin et al. 2010) is devoted primarily to spectral line surveys. One of the sources studied is Sagittarius B2(N)—a line of sight that shows a rich, complex molecular emission and absorption spectrum (Fig. 1).

Hydronium is an important molecular ion in the oxygen molecular network (e.g., Phillips et al. 1992 and references therein). It is isoelectronic with ammonia, like ammonia is a symmetric rotor, and it also has the characteristic inversion

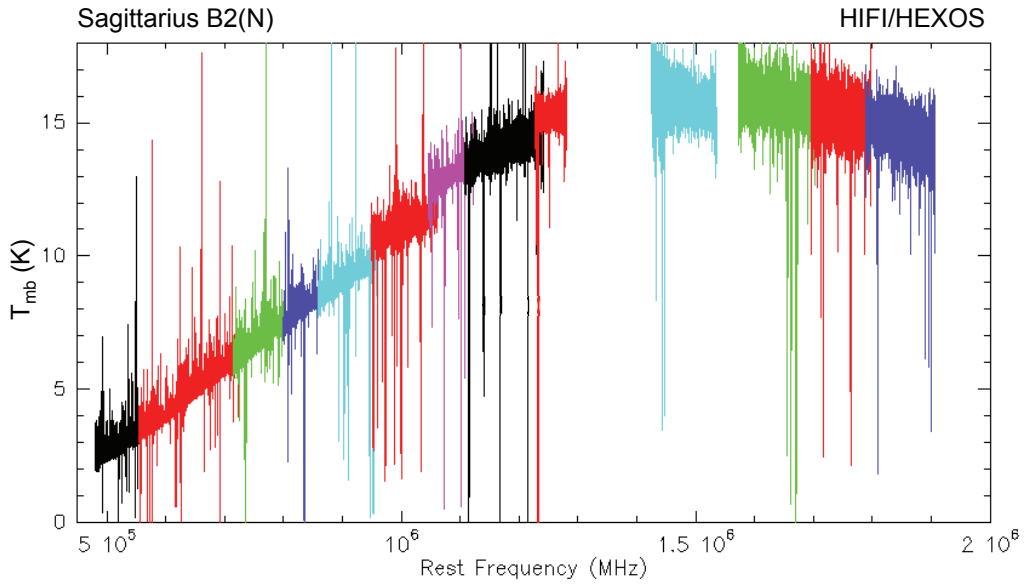

Figure 1. Herschel/HIFI spectral scan of Sagittarius B2(N). A complex spectrum of emission and absorption features is seen, with absorption dominating the spectrum above about 1 THz. The HIFI point source sensitivity is 464–506 Jy/K at frequencies 480–1910 GHz and the FWHM beam size varies between 44″ and 11″, respectively. (Online version in colour.)

splitting of its rotational levels. However, in the case of H_3O^+ the inversion splitting is very large, comparable to the rotational level spacing, and lines occur in the THz frequency range (Liu & Oka 1985; see the energy level diagram in Fig. 2). Just like in the case of ammonia, H_3O^+ has *ortho* and *para* spin variants. Levels with $K = 0$ and $3n$ are *ortho* and those with $K = 3n + 1$ and $3n + 2$ *para*. Since there are no allowed radiative transitions between different K ladders, the lowest energy levels in each ladder are metastable, connected only by collisions, and their relative populations can be used to derive an estimate of the gas kinetic temperature (e.g., Danby et al. 1988; Maret et al. 2009 for NH_3). Transitions connecting to these metastable levels are referred to here as "metastable transitions".

2. Observations

Herschel/HIFI observations presented here were carried out between 2010 September and 2011 April, using the HIFI single point dual beam switch (DBS) observing mode. The source coordinates are: $\alpha_{J2000} = 7^{\rm h}47^{\rm m}19\overset{\rm s}{.}88$, $\delta_{J2000} = -28°22'18\overset{''}{.}4$. The DBS reference beams lie approximately 3′ east and west (i.e. perpendicular to the roughly north-south elongation of the source). We used the HIFI wide band spectrometer (WBS) providing a spectral resolution of 1.1 MHz over a 2.5 GHz IF bandwidth of the high-frequency HEB receivers. The spectra presented here are averages of the H and V polarizations, with equal weighting,

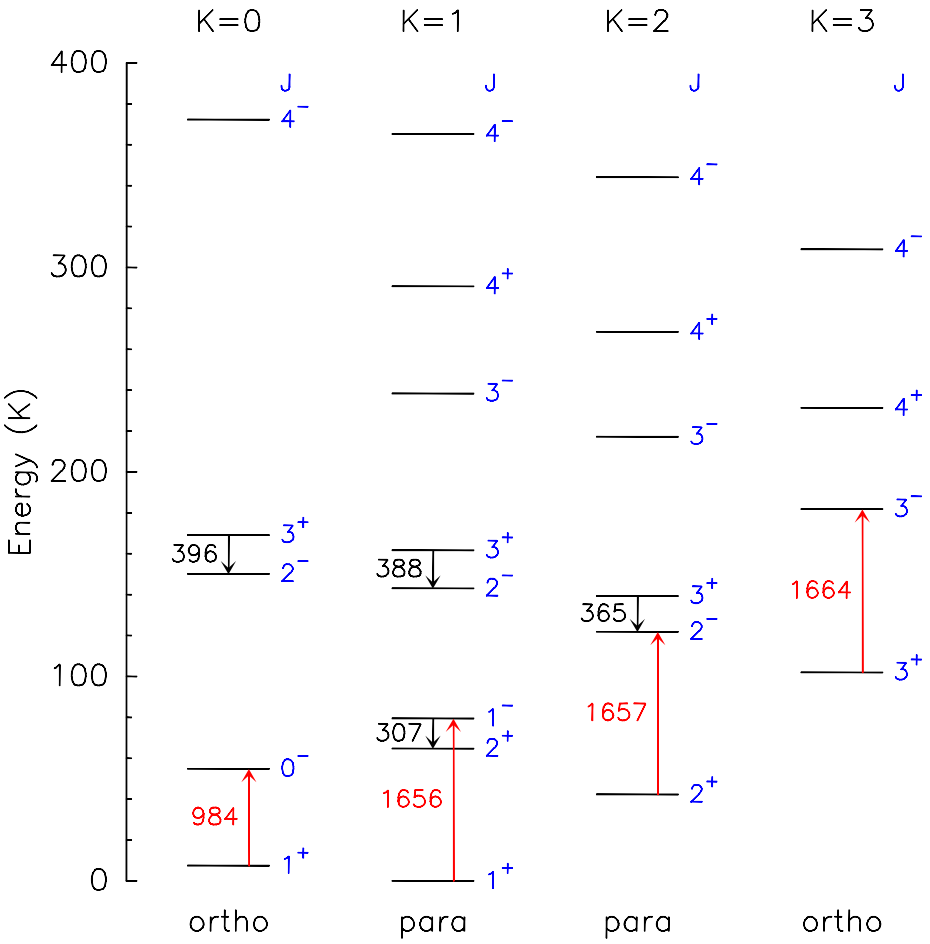

Figure 2. H_3O^+ energy level diagram. Transitions connecting to the ground state level in each K ladder, which are discussed in this paper, are marked in red. Other millimeter-wave transitions previously studied from the ground are marked in black (these are typically seen in emission). Transitions are labeled with the corresponding line frequency in GHz. The "+" and "−" signs denote parity of the levels. All levels for which collisional rates are available in the LAMDA database (www.strw.leidenuniv.nl/ñoldata/) are included in the figure. (Online version in colour.)

reduced using HIPE (Ott 2011) with pipeline version 5.1. The double sideband spectra were subsequently deconvolved into single sideband spectra using the technique described in Comito & Schilke (2002).

3. Discussion

The H_3O^+ absorption spectra towards Sagittarius B2(N) are shown in Figure 3. Metastable transitions up to (11,11), with a lower level energy of 1219 K, are covered in the HIFI spectra and clear signatures of H_3O^+ absorption are detected.

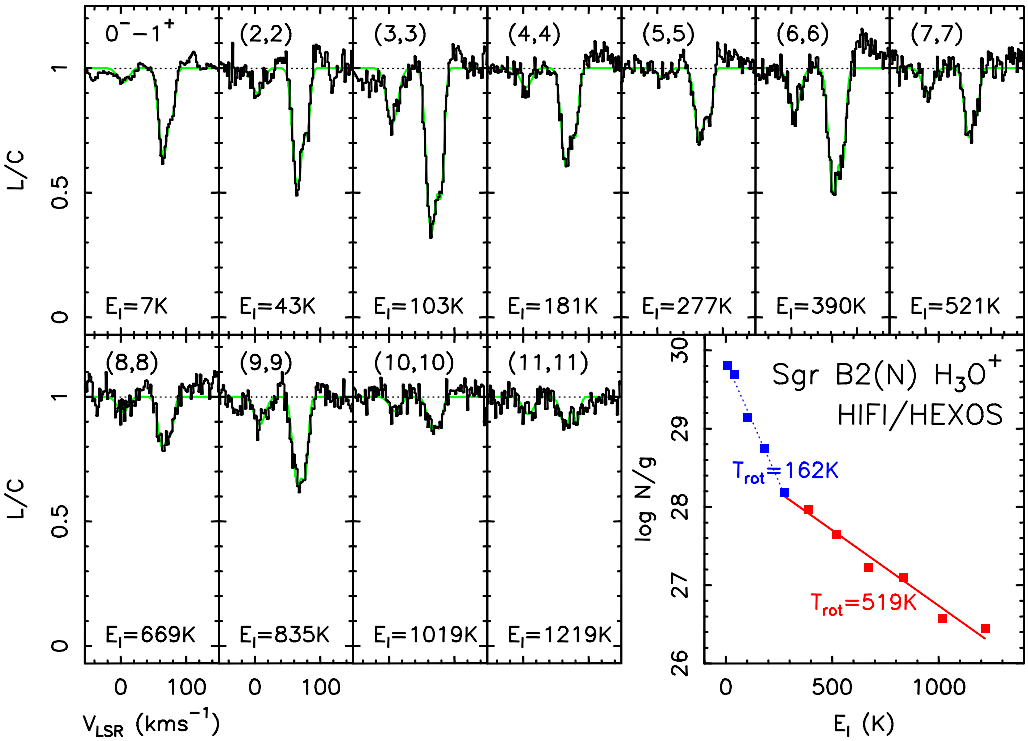

Figure 3. Spectra of H_3O^+ absorption towards Sgr B2(N), normalized to the continuum. The 0^-–1^+, (3,3) , (6,6), and (9,9) lines are *ortho* and the remaining lines are *para*. The (1,1) line is blended with the $2_{1,2}$–$1_{0,1}$ transition of $H_2^{18}O$ and cannot be used in the analysis. *(Lower-right)* The H_3O^+ population diagram for the sum of the 65 and 80 km s^{-1} components. An LTE *ortho*/*para* ratio of 3:1 is assumed. (Online version in colour.)

The (1,1) ground state *para* transition at 1655.831 GHz is blended with the $2_{1,2}$–$1_{0,1}$ transition of $H_2^{18}O$ at 1655.868 GHz and cannot be used in the excitation analysis. However, all the remaining metastable transitions, as well as the ground state 0^-–1^+ *ortho* line at 984.709 GHz, are clean from line contamination.

Figure 4 shows a uniformly-weighted average of the H_3O^+ (2,2) to (11,11) metastable transitions, with lower level energies greater than 43 K, (*a*), and the H_3O^+ 0^-–1^+ transition (*b*; shifted down by 0.4 to avoid overlap). At least four H_3O^+ absorption components can be identified in the averaged spectrum of the metastable transitions, with central LSR velocities of −75, 6, 65, and 80 km s^{-1}. The first two velocity components correspond to foreground gas on the line of sight, but still in the Galactic Center region, while the later two are associated with the Sagittarius B2 cloud itself. The 65 km s^{-1} component is also seen towards the nearby source Sagittarius B2(M), while the 80 km s^{-1} component is local to Sagittarius B2(N). Although the signal-to-noise of the top spectrum is limited, it appears that −104 and −40 km s^{-1} components, which are quite prominent in other molecular tracers, such as ammonia (Fig. 4 *c*, shifted down by 0.8), are weak or absent in the metastable H_3O^+ transitions. However, weak absorption at these velocities can be seen in H_3O^+ 0^-–1^+ spectrum Figure 4 (*b*)—in this case the

absorption originates from the ground state *ortho*-H_3O^+ level. Figure 4 (*d*; red curve) shows a spectrum of H_3^+ R(1,1)^l absorption at 3.715 μm on a nearby line of sight, 2M1747, between Sagittarius B2 and Sagittarius B1 (Geballe & Oka 2010). All the velocity components seen in the metastable H_3O^+ transitions can also be identified in the H_3^+ spectrum which shows, however, many additional velocity components—notably, the strongest H_3^+ absorption is seen at -40 km s^{-1}, which comes from the 3 kpc arm (Vallée et al. 2008), outside the Galactic Center. The differences between the H_3^+ and H_3O^+ absorption patterns may be partly due to the limited signal-to-noise ratio of the high-frequency HIFI spectra. However, it appears that H_3O^+ is strongly enhanced only in some of the H_3^+ velocity components.

The H_3O^+ population diagram for the sum of the 65 and 80 km s^{-1} components is shown in Figure 3, lower-right panel. It can be described by a two-component model, with rotational temperatures of 162 and 519 K, respectively. The total H_3O^+ column density in the hot component is estimated to be 4×10^{14} cm^{-2}.

The detection of H_3O^+ absorption in multiple metastable transitions, with lower level energies up to $\sim$1200 K, is surprising. Earlier Herschel/HIFI observations towards W31C and W49N, outside of the Galactic center (Gerin et al. 2010; Neufeld et al. 2010; see also Gerin et al, this volume) have shown strong OH^+ and H_2O^+ absorption, but only weak H_3O^+. These observations probe primarily diffuse gas, with low molecular fractions. Neufeld et al. (2010) argue that if the ratio of electron density to H_2 is sufficiently large, the pipeline leading from O^+ to OH^+, to H_2O^+, to H_3O^+ can be leaky, with the flow of ionization reduced at each step by the dissociative recombination of OH^+ and H_2O^+. In dense molecular clouds, by contrast, the ionized hydrogen abundance and temperature are both too small for O^+ production by charge transfer to be efficient, and the dominant source of OH^+ is the reaction of H_3^+ with O. Once again, the chemistry is driven by cosmic ray ionization—the original source of H_3^+—but now the conversion of OH^+ to H_2O^+, to H_3O^+ via reactions with H_2 proceeds with almost 100 % efficiency. In this context, the non-detection of H_3O^+ towards Orion KL by Gupta et al. (2010) is interesting. On this line of sight, the column densities of the three oxygen-bearing ions are up to an order of magnitude lower than those towards W31C and W49N. These comparatively low column densities may be explained by a higher gas density, despite the assumption of a very high ionization rate.

The sightline towards Sagittarius B2 is different from the sightlines previously studied by HIFI in that it probes the molecular gas in the Central Molecular Zone, characterized by higher density, degree of turbulence, as well as increased rates of cosmic ray and X-ray fluxes (e.g., Morris & Serabyn 1996)—the environment typically found in active galactic nuclei. Below, we discuss how these factors may affect H_3O^+ column density and excitation.

(*a*) *Shocks*

Ceccarelli et al. (2002) carried out an unbiased spectral scan towards Sagittarius B2 using the ISO Long Wavelength Spectrometer (LWS) and detected absorption signatures of 21 ammonia transitions covering a wide range of energy levels between 65 and 720 K, including metastable and non-metastable levels

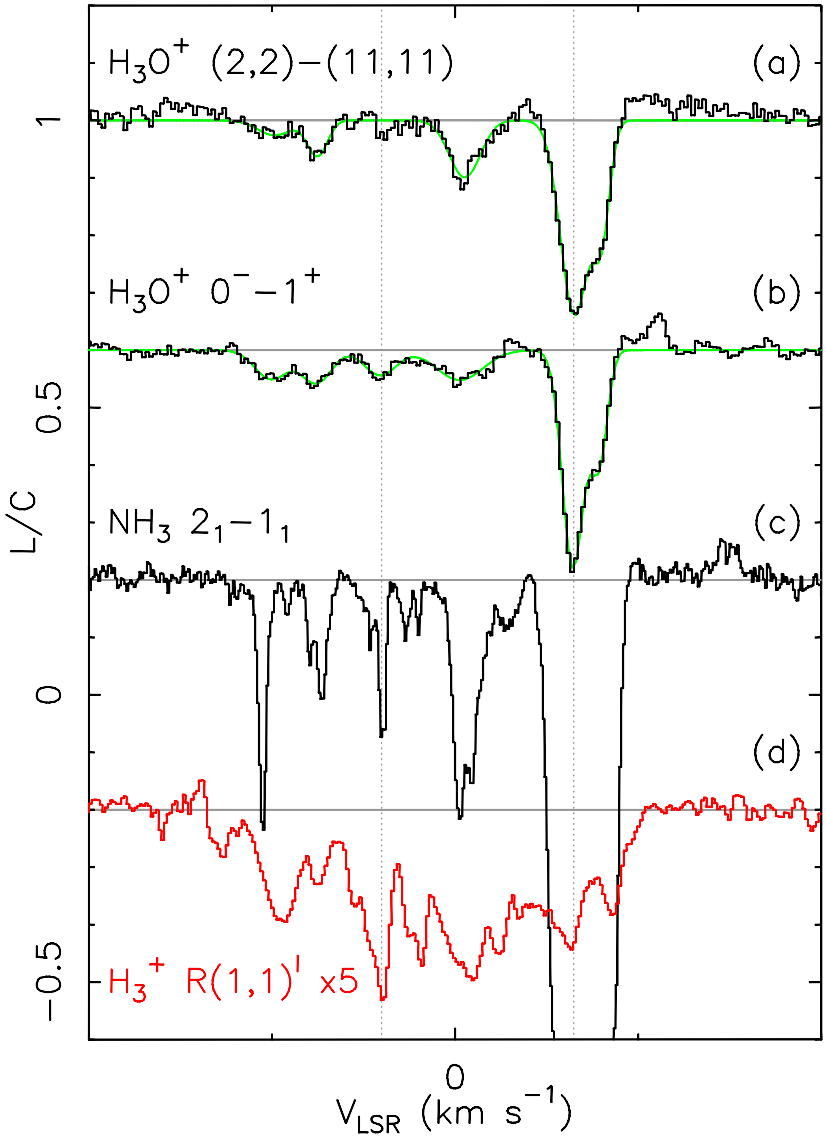

Figure 4. (a) A uniformly-weighted average of the H_3O^+ (2,2) to (11,11) spectra; (b) the H_3O^+ 0^-–1^+ spectrum; (c) the 2_1–1_1 spectrum of *para*-NH_3 towards Sagittarius B2(N); and (d) the $R(1,1)^l$ spectrum of H_3^+ (multiplied by 5; Geballe & Oka, 2010) for a nearby line of sight, 2M1747, between Sagittarius B2 and Sagittarius B1. The four spectra have been shifted vertically to avoid overlap. Green lines shows multicomponent Gaussian fits to the H_3O^+ spectra. The strong 3_{11}–2_{10} line of NH_3, present in the (9,9) spectrum at about -110 km s^{-1}, has been removed before averaging the spectra of the metastable transitions. Spectra of OH^+ and H_2O^+ on the same line of sight are also available, but not shown here, because complex hyperfine patterns do not allow to easily isolate individual velocity components. (Online version in colour.)

of both *ortho* and *para* species. They concluded that the absorption occurs in a thin, hot foreground layer, with a kinetic temperature of 700 ± 100 K and a

density of $\sim 10^4$ cm^{-3}. Earlier ground-based observations of the ammonia inversion lines at radio wavelengths (e.g., Hüttemeister et al. 1995, Flower et al. 1995) have been explained by the presence of shocked gas on the line of sight towards Sagittarius B2[1] and the ISO LWS observations of Ceccarelli et al. (2002) are consistent with this explanation. The angular extent of the absorbing layer is estimated to be $\sim 30''$ (although the 60 km s^{-1} component is seen towards both N and M sources, which are separated by $45''$). Assuming an ammonia abundance of 10^{-6} (appropriate for shocked gas, but highly uncertain), the corresponding H_2 column density in the hot layer is $\sim 3 \times 10^{22}$ cm^{-2}.

The rotational temperature of hot H_3O^+ towards Sagittarius B2 is consistent with the earlier ammonia estimates. A natural explanation would thus be that H_3O^+ comes from the same shocked layer as ammonia. In this case, the H_3O^+ abundance would be 1.3×10^{-8}. However, the main source of ionization in shocks are UV photons (J-shocks only) and models have shown that the H_3O^+ abundance in UV irradiated regions does not exceed 3×10^{-9}, even for extreme cosmic ray ionization rates (5×10^{-15} s^{-1}; e.g., van der Tak et al. 2008). A detailed analysis of the H_3O^+ excitation under the conditions characteristic of the shocked layer is hampered by the lack of collisional cross-sections, which are available only for the low-energy H_3O^+ rotational levels shown in Figure 2.

The kinematics of the hot layer poses another intriguing question, as the velocities of the absorbing components are the same as those of the dense cores in Sagittarius B2, while low-density gas is present throughout the cloud envelope over a wide range of velocities, between 0 and 100 km s^{-1}. This and the small angular extent derived from ISO observations indicate that the absorbing gas may be associated with the region in the immediate vicinity of the dense cores. Rolffs et al. (2010) have detected signatures of the reversal of infall in Sagittarius B2(M) in ground-based and HIFI spectra of HCN transitions, with infall dominating in the colder, outer regions, and expansion dominating in the warmer, inner regions. It is possible that a shock may be present at the interface between these two regimes. However, one would then expect a much higher density in the shocked gas than that derived from the ammonia observations.

Wirström et al. (2010) have modeled *Odin* observations of water and ammonia absorption lines towards Sagittarius B2 and concluded that the non-LTE excitation of ammonia in the environment of Sagittarius B2 could be explained without invoking a hot molecular layer in addition to the warm envelope gas, but no details are given. In addition, a hot layer is also not required to explain the line profiles of water isotopologues observed by *Odin*.

(*b*) *Cosmic rays*

In a recent study Meijerink et al. (2011) modeled the effect of cosmic rays and mechanical heating on molecular abundances in environments characteristic of active galactic nuclei. In the Meijerink et al. (2011) models, the H_3O^+ abundance can reach values as high as 1×10^{-8} at hydrogen column densities in excess of 1×10^{22} cm^{-2}, but only for relatively high gas densities (a few $\times 10^5$ cm^{-3}). The H_3O^+/H_2O ratio predicted by these models is typically $\sim 10^{-2}$. The H_2O

[1] A large-scale shock in Sagittarius B2, caused by a cloud cloud collision, has also been postulated by Hasegawa et al. (1994), based on the observed morphology and kinematics of ^{13}CO emission.

column density towards Sagittarius B2 in the relatively large SWAS beam is $\sim 2.4 \times 10^{16}$ cm^{-2} (Comito et al. 2003). The observed H_3O^+/H_2O ratio is thus in the correct range. The high gas density required to produce the enhanced H_3O^+ abundances is consistent with that present in the central 5×10 pc core of Sagittarius B2 (e.g., Lis & Goldsmith 1991), but again appears inconsistent with the value derived for the hot ammonia layer.

(*c*) *X-rays*

X-rays can easily create H_3O^+ via reaction of H_3^++O, followed by H_2O^++H_2, or by H_3^++H_2O, and models suggest that H_3O^+ abundances in excess of 10^{-8} and beyond are likely to occur in XDRs (van der Tak et al. 2008). It is also straightforward to obtain H_3O^+/H_2O ratios as high as 10^{-2} in XDRs, while PDR model ratios are generally 10^{-3} or less. The H_3O^+ abundance and the H_3O^+/H_2O ratio towards Sagittarius B2 are thus in the range predicted by XDR models.

The presence of strong 6.4 keV iron fluorescence and hard X-ray emission has lead to the suggestion that giant molecular clouds in the Galactic center, in particular Sagittarius B2, have been recently illuminated by an X-ray flash (Sunyayev et al. 1993; Koyama et al. 1996). Terrier et al. (2010) have shown clear observational evidence that the X-ray emission of Sagittarius B2 is now fading. The characteristic time scale for the decay is $\sim$8 yr, compatible with the light crossing time of the molecular cloud core. Based on this fast variability, Terrier et al. (2010) rule out alternative explanations of the origin of the iron line and continuum emission, such as inverse bremsstrahlung from sub-relativistic ions and low-energy cosmic ray electrons, and conclude that Sagittarius B2 is likely an X-ray reflection nebula. The location of the illuminating source is yet to be determined, but the most likely explanation is a period of high activity of the massive black hole at the center of the Galaxy, associated with the radio continuum source Sagittarius A*, which ended about 100 years ego.

X-ray driven chemistry thus offers an interesting explanation for the observed hot, metastable H_3O^+ towards Sagittarius B2. In the context of X-ray models, the high rotational temperature observed may be naturally explained by the H_3O^+ formation pumping—H_3O^+ molecules are formed in highly excited states, and quickly decay radiatively to populate the metastable levels probed by our HIFI observations. The reaction H_2O^++H_2→H_3O^++H has an exothermicity of 1.694 eV and H_3^++H_2O→H_3O^++H_2 of 2.814 eV. It is not known how this excess energy is distributed between the reaction products and one may expect that the light H and H_2 carry most of the excess energy. However, in principle a lot of excess energy is available to populate excited H_3O^+ levels. The population would then get trapped in the metastable levels that are probed by our HIFI observations.

While this explanation is appealing, given our understanding of the physical conditions in the Sagittarius B2 environment, detailed model calculations are required, as formation pumping is relatively inefficient. While XDR models may be able to easily reproduce the required column density of H_3O^+, explaining the observed excitation requires that the collisional relaxation time is long relative to that required for recombination/reformation of H_3O^+ molecules (molecules have to be produced efficiently in highly-excited states before they have time to relax through collisions and typical reaction rates are of order 10^{-9} s^{-1}, only a factor of a few larger than typical collisional de-excitation rates). Ammonia observations

would also have to be explained by the same model and one may expect that ammonia, being chemically more stable than H_3O^+, would have more time to relax through collisions, and should thus display a lower rotation temperature.

(*d*) *Extragalactic* H_3O^+

The Galactic Center can be viewed as the closest active galactic nucleus. In this context our observations are relevant for extragalactic applications. Aalto et al. (2011) have observed H_3O^+ towards the centers of seven active galaxies to investigate the impact of starburst and AGN activity on the chemistry of the interstellar medium. They find high H_3O^+ abundances, in excess of 10^{-8}, in four galaxies: NGC 253, NGC 1068, NGC 4418, and NGC 6240. Only in IC 342, the H_3O^+ abundance is an order of magnitude lower and here a standard PDR chemistry can explain the observed H_3O^+ abundance. The temperature of the H_3O^+ emitting gas is not constrained by the present observations. While the large H_3O^+ columns derived towards the four galaxies are generally consistent with predictions of XDR models, Aalto et al. (2011) also consider an alternative scenario, in which H_3O^+ can be formed from H_2O evaporating from dust grains and reacting with HCO^+ in warm, dense gas. Shocks would help remove water molecules from grain mantles. Detailed modeling of the H_3O^+ excitation towards Sagittarius B2, in conjunction with HIFI observations of water isotopologues on the same line of sight, may help distinguish between these scenarios. We note, however, that earlier SWAS and HIFI observations (Neufeld et al. 2000; Lis et al. 2010) indicate enhanced water abundance on the line of sight toward Sagittarius B2.

4. Concluding remarks

The H_3O^+ results presented here should be considered preliminary, as significant improvements are expected for the pipeline processing of the HIFI HEB bands in the recently released version 8 of the HIPE software. The resulting improvement in the SNR in the spectra should increase the accuracy of the population diagrams and possibly allow the determination of the rotation temperature for the individual velocity components in the H_3O^+ absorption spectra (Fig. 4).

H_3O^+ formation pumping in X-ray irradiated gas seems to naturally explain our observations, but detailed models are needed to support this hypothesis and exclude alternative explanations, such as shocks or cosmic rays. Given the observed decrease in the X-ray flux, these models should naturally be time dependent and should explain simultaneously both the hydronium ion and ammonia observations.

Acknowledgment

We thank E. Roueff and T. Oka for helpful comments. HIFI has been designed and built by a consortium of institutes and university departments from across Europe, Canada and the United States under the leadership of SRON Netherlands Institute for Space Research, Groningen, The Netherlands and with major contributions from Germany, France and the

US. Consortium members are: Canada: CSA, U. Waterloo; France: CESR, LAB, LERMA, IRAM; Germany: KOSMA, MPIfR, MPS; Ireland, NUI Maynooth; Italy: ASI, IFSI–INAF, Osservatorio Astrofisico di Arcetri–INAF; Netherlands: SRON, TUD; Poland: CAMK, CBK; Spain: Observatorio Astronmico Nacional (IGN), Centro de Astrobiologa (CSIC–INTA). Sweden: Chalmers University of Technology–MC2, RSS & GARD; Onsala Space Observatory; Swedish National Space Board, Stockholm University–Stockholm Observatory; Switzerland: ETH Zurich, FHNW; USA: Caltech, JPL, NHSC. Support for this work was provided by NASA through an award issued by JPL/Caltech.

References

Aalto, S., Costafliola, F., van der Tak, F., & Meijerink, R. 2011 H_3O^+ line emission from starbursts and AGNs. *Astron. & Astroph.* **527**, A69.

Bergin, E. A., Phillips, T. G., Comito, C., et al. 2010 Herschel observations of EXtra-Ordinary Sources (HEXOS): The Terahertz spectrum of Orion KL seen at high spectral resolution. *Astron. & Astroph.* **521**, L21.

Ceccarelli, C., Baluteau, J.-P., Walmsley, M., et al. 2002 ISO ammonia line absorption reveals a layer of hot gas veiling Sgr B2. *Astron. & Astroph.* **383**, 603–613.

Comito, C., & Schilke, P. 2002 Reconstructing reality: Strategies for sideband deconvolution. *Astron. & Astroph.*, **395**, 357–371.

Comito, C., Schilke, P., Gerin, M., et al. 2003 The line-of-sight distribution of water in the SgrB2 complex. *Astron. & Astroph.* **402**, 635–645.

Danby, G., Flower, D. R., Valiron, P., Schilke, P., & Walmsley, C. M. 1988 A recalibration of the interstellar ammonia thermometer. *Mon. Not. R. Astr. Soc.*, **235**, 229–238.

Flower, D. R., Pineau des Forêts, G., & Walmsley, M. 1995 Hot shocked ammonia towards Sgr B2. *Astron. & Astroph.* **294**, 815–824.

de Graauw, Th., Helmich, F., Phillips, T. G., et al. 2010 The Herschel-Heterodyne Instrument for the Far-Infrared (HIFI). *Astron. & Astroph.* **518**, L6.

Geballe, T., & Oka, T. 2010 Two new and remarkable sightlines through the Galactic Center's molecular gas. *Astroph. J.* **709**, L70–L73.

Gerin, M., De Luca, M., Black, J., et al. 2010 Interstellar OH^+, H_2O^+ and H_3O^+ along the sight-line to G10.6-0.4. *Astron. & Astroph.* **518**, L110.

Gupta, H., Rimmer, P., Pearson, J. C., et al. 2010 Detection of OH^+ and H_2O^+ towards Orion KL. *Astron. & Astroph.* **521**, L147.

Hasegawa, T., Sato, F., Whiteoak, J. B., & Miyawaki, R. 1994 A Large Scale Cloud Collision in the Galactic Center Molecular Cloud Near Sagittarius B2. *Astroph. J.* **429**, L77–L80.

Hüttemeister, S., Wilson, T.L., Mauersberger, R., et al. 1995 A multilevel study of ammonia in star-forming regions: VI. The envelope of Sagittarius B2. *Astron. & Astroph.* **294**, 667–676.

Koyama, K., Maeda, Y., Sonobe, T., et al. 1996 ASCA View of Our Galactic Center: Remains of Past Activities in X-Rays? *Publ. Astron. Soc. Japan* **48**, 249–255.

Lis, D.C., & Goldsmith, P.F. 1991 High-Density Gas in the Core of the Sagittarius B2 Molecular Cloud. *Astroph. J.* **369**, 157–168.

Lis, D.C., Phillips, T.G., Goldsmith, P.F., et al. 2010 Herschel/HIFI measurements of the ortho/para ratio in water towards Sagittarius B2(M) and W31C. *Astron. & Astroph.* **521**, L26.

Liu, D.-J., & Oka, T. 1985 Experimental Determination of the Ground-State Inversion Splitting in H_3O^+. *Phys. Rev. Lett.* **54**, 1787–1789.

Maret, S., Faure, A., Scifoni, E., & Wiesenfeld, L. 2009 On the robustness of the ammonia thermometer. *Mon. Not. R. Astr. Soc.*, **399**, 425–431.

Meijerink, R., Spaans, M., Loenen, A. F., & van der Werf, P. P. 2011 Star formation in extreme environments: the effects of cosmic rays and mechanical heating. *Astron. & Astroph.* **525**, A119.

Morris, M., & Serabyn, E. 1996 The Galactic Center Environment. *Ann. Rev. Astron. Ap.* **34**, 645–702.

Neufeld, D. A., Ashby, M. L. N., Bergin, E. A., et al. 2000 Observations of Absorption by Water Vapor toward Sagittarius B2. *Astroph. J.* **539**, L111.

Neufeld, D. A., Goicoechea, J. R., Sonnetrucker, P., et al. 2010 Herschel/HIFI observations of interstellar OH^+ and H_2O^+ towards W49N: a probe of diffuse clouds with a small molecular fraction. *Astron. & Astroph.* **518**, L10.

Ott, S. 2011 HIPE, HIPE, Horray! In Astronomical Data Analysis Software and Systems XIX, ed. Y. Mizumoto, K.-I. Morita, & M. Ohishi, *ASP Conf. Ser.*, **442**, 347.

Pilbratt, G. L., Riedinger, J. R., Passvogel, T., et al. 2010 Herschel Space Observatory. An ESA facility for far-infrared and submillimetre astronomy. *Astron. & Astroph.* **518**, L1.

Phillips, T. G., van Dishoeck, E. F., & Keene, J. B. 1992 Interstellar H_3O^+ and its relationship to the O_2 and H_2O abundances. *Astroph. J.* **399**, 533–550.

Rolffs, R., Schilke, P., Comito, C., et al. 2010 Reversal of infall in Sgr B2(M) revealed by Herschel HIFI observations of HCN lines at THz frequencies. *Astron. & Astroph.* **521**, L146.

Sunyaev, R. A., Markevitch, M., & Pavlinsky, M. 1993 The Center of the Galaxy in the Recent Past: A View from GRANAT. *Astroph. J.* **407**, 606–610.

Terrier, R., Ponti, G., Bélanger, G., et al. 2010 Fading Hard X-ray Emission from the Galactic Center Molecular Cloud Sgr B2. *Astroph. J.* **719**, 143–150.

Vallée, J. P. 2008 An Improved Magnetic Map of the Milky Way, with the Circularly Orbiting Gas and Magnetic Field Lines Crossing the Dusty Stellar Spiral Arms. *Astronom. J.*, **135**, 303–310.

van der Tak, F.F.S., Aalto, S., & Meijerink, R. 2008 Detection of extragalactic H_3O^+. *Astroph. J.* **477**, L5–L8.

Wirström, E. S., Bergman, P., Black, J. H., et al. 2010 Ground-state ammonia and water in absorption towards Sgr B2. *Astron. & Astroph.* **522**, A19.